Nuclear Weak Processes and Astrophysical Applications

Toshio Suzuki[1,2] **and Michio Honma**[3]

[1]Department of Physics, College of Humanities and Sciences, Nihon University
Sakurajosui 3-25-40, Setagaya-ku, Tokyo 156-8550, Japan
[2]Center for Nuclear Study, University of Tokyo, Hirosawa, Wako-shi, Saitama 351-0198, Japan
[3]Center for Mathematical Sciences, University of Aizu
Aizu-Wakamatsu, Fukushima 965-8580, Japan

E-mail: suzuki@chs.nihon-u.ac.jp

Abstract. Nuclear weak processes are investigated based on new shell model Hamiltonians, which give successful description of spin responses in nuclei, and applied to astrophysical problems. Neutrino-induced reactions on ^{12}C and synthesis of light elements by supernova neutrinos, and effects of contamination of ^{13}C, whose natural isotopic abundance is 1.1%, on inclusive ν-^{12}C reactions are discussed. Spin-dipole transitions and ν-induced reactions on ^{16}O are studied by using a new Hamiltonian with proper tensor components, and compared with conventional calculations and previous CRPA results. Gamow-Teller transition strength in ^{40}Ar and ν-induced reactions on ^{40}Ar by solar neutrinos are studied based on monopole-based-universal interaction (VMU). We finally discuss electron capture reactions on Ni isotopes in stellar environments.

1. Introduction

Neutrino-nucleus reactions and electron capture reactions, which are dominantly induced by excitations of spin modes in nuclei, are investigated with the use of new shell model Hamiltonians, SFO[1] and SFO-tls [2] in p-shell and p-sd shell, GXPF1 [3] in fp-shell and monopole-based-universal interaction (VMU[4]) in sd-fp shell. The new Hamiltonians properly take into account important roles of the tensor interactions.

Neutrino nucleus reactions on ^{12}C, ^{13}C and ^{16}O are studied in Sect. 2. Neutrino-induced reactions on ^{40}Ar are studied in Sect. 3. Electron capture reactions on Ni isotopes in stellar environments are discussed in Sect. 4.

2. Neutrino-Nucleus Reactions in Carbon and Oxygen

2.1. Neutrino-induced Reaction on ^{12}C and Light Element Synthesis

Neutrino-induced reactions in p-shell nuclei are investigated based on new shell model Hamiltonians[1], which take into account important roles of tensor interaction properly[9] and give good account of spin-dependent modes in p-shell nuclei. Magnetic moments of p-shell nuclei are systematically well described, and Gamow-Teller (GT) transition strengths in ^{12}C and ^{14}C are also well explained[1].

The GT strength in ^{12}C is enhanced for the new Hamiltonian, SFO[1], compared to conventional Hamiltonians, and the cross sections of ν-induced exclusive charge-exchamge reaction, ^{12}C (ν, e^-) ^{12}N$_{g.s.}$, are reproduced by SFO. The enhancement of the ν-^{12}C reaction cross sections is found to lead to the enhancement of the production yields of light elements, ^{11}B and ^{7}Li, in supernova explosions[5, 6]. The element ^{11}B is produced by both ^{12}C (ν, ν'p) ^{11}B and ^{7}Li (α, γ) ^{11}B reactions while ^{7}Li is produced through ^{4}He (ν, ν'p) ^{3}H (α, γ) ^{7}Li. Therefore, in addition to the enhancement of the reaction cross sections in ^{12}C, the enhancement of the ν-^{4}He reaction cross sections with the use of recent Hamiltonians such as WBP[7] is also important to get the enhancement of the enhancemrnt of the production yields of ^{7}Li and ^{11}B. The enhancement factor for the production yield is found to be about 20% and 30% for ^{11}B and ^{7}Li, respectively, for WBP+SFO Hamiltonians in a supernova explosion explosion model[5]. Here, neutral current reactions induced by heavy-flavor neutrinos with higher energies play dominant roles, while in case of neutrino oscillations charge-exchange reactions induced by ν_e also become important[6].

2.2. Neutrino-induced Reactions on ^{13}C

Neutrino-induced reactions on ^{13}C are studied by shell model calculations with the use of SFO. The carbon target is one of a very few examples, on which neutrino induced reactions are measured. The target is usually assumed to be pure ^{12}C isotope while it has contamination of ^{13}C with 1.1% of the natural isotopic abundance. As the Q-values for the ν-^{13}C reactions are low compared to ^{12}C case, the cross sections for ^{13}C are larger than those of ^{12}C and the small admixture of ^{13}C in the target can have non-negligible contributions to the inclusive ν-carbon cross sections at low neutrino energies.

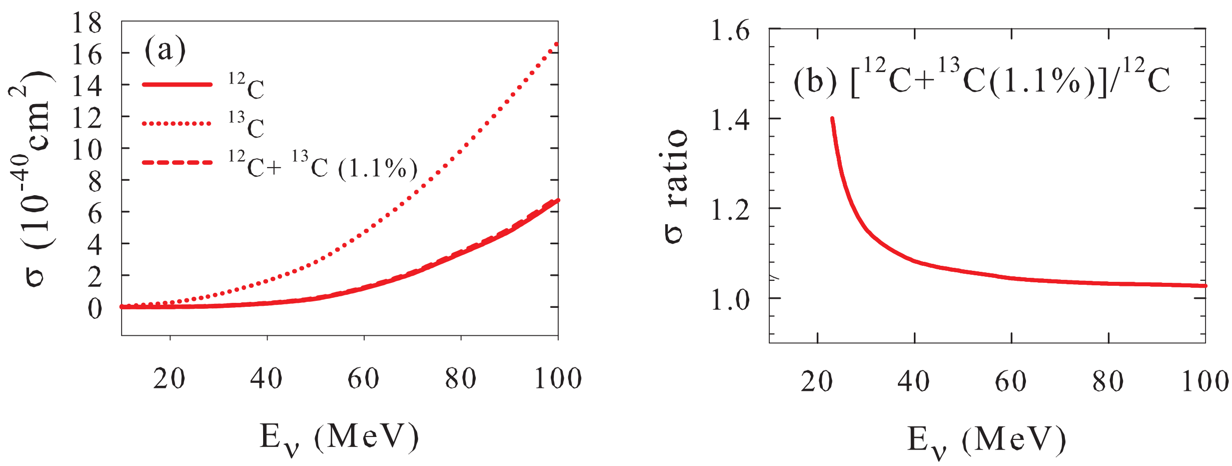

Figure 1. (a) Inclusive reaction cross sections for ^{12}C (ν, e^-) ^{12} and ^{13}C (ν, e^-) ^{13}N obtained by shell model calculations with the use of SFO. The sum of ^{12}C and 1.1% of ^{13}C cross sections are also shown. (b) Ratio of the cross sections; [^{12}C + ^{13}C (1.1%)]/^{12}C.

Calculated inclusive cross sections for carbon isotopes are shown in Fig. 1. The contributions from GT and spin-dipole transitions are included; multipoles up to J^{π} = $4^{\pm}$ are taken into account. The effects of the mixing of ^{13}C on the ν-^{12}C cross sections are about 20% ∼4% at E_ν =30∼80 MeV, and get larger at lower E_ν (see Figs.1(a) and 1(b)). The inclusive cross sections for supernova temperatures T_ν are affected by about 30% ∼5% at T_ν =4∼10 MeV. While the effects are minor at high temperatures, they can be as large as (50%, 30%, 15%) for T_ν =(3.5, 4, 6) MeV, which correspond to a typical set of T_ν for (ν_e, $\bar{\nu}_e$, $\nu_{\mu,\tau}$ and $\bar{\nu}_{\mu,\tau}$).

2.3. Neutrino-induced Reactions on ^{16}O

The ^{16}O nucleus plays an important role in producing ^{15}N by ^{16}O (ν, ν'p) ^{15}N reaction in supernova explosions. It is also contained in water, which is used as target for neutrino detections, Here, ν-^{16}O reactions are studied by using the modified SFO interaction, SFO-tls[2], where the tensor components of the $\pi + \rho$ -meson exchange potential are used for the *p*-*sd* cross shell two-body matrix elements. As the ν-^{16}O reactions are mainly induced by spin-dipole transitions, it is important to take full account of the tensor force properly in the *p*-*sd* cross shell part. Energies of the spin-dipole states are rather well reproduced. Calculated spin-dipole strength is more fragmented and shifted toward lower energy region for SFO-tls compared to SFO.

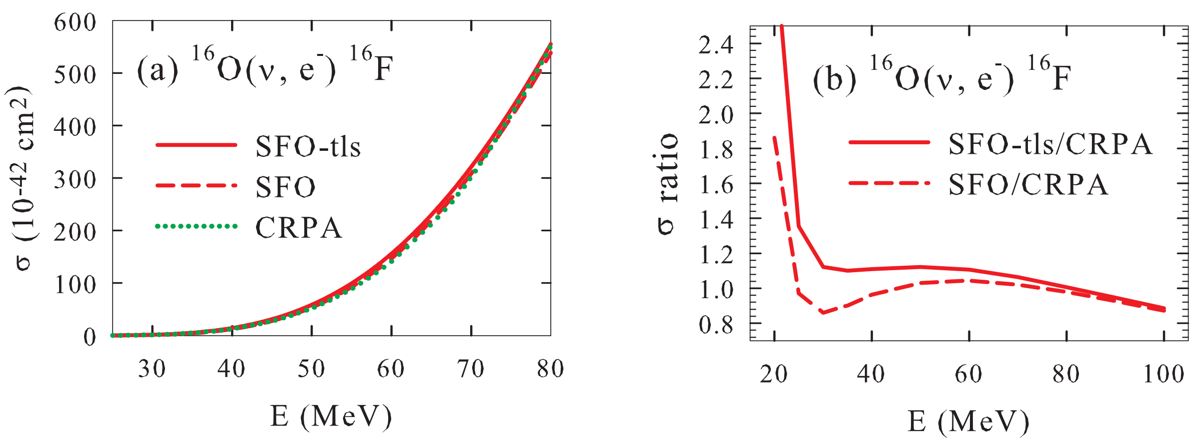

Figure 2. (a) Calculated reaction cross sections for ^{16}O (ν, e^-) ^{16}F obtained by shell model calculations with the use of SFO-tls and SFO, as well as CRPA calculations. (b) Ratios of the cross sections; SFO-tls vs CRPA, and SFO vs CRPA.

Calculated cross sections for charged-current and neutral-current reactions are shown in Figs. 2 and 3, respectively. The cross sections obtained by SFO-tls are compared with those of SFO and CRPA[8]. The charged-current (neutral-current) cross sections for SFO-tls are enhanced compared with those of SFO and CRPA by about 30% ∼5% (20% ∼10%) and 15%, respectively, at E_ν =30∼60 MeV. It would be interesting to study effects of the enhancement of the cross sections for SFO-tls on nucleosynthesis and neutrino detections.

3. Neutrino-induced Reactions on ^{40}Ar

Liquid Ar is an important target to measure solar neutrinos. Neutrino-induced reactions on ^{40}Ar are studied by using the monopole-based-universal interaction (VMU) which has proper tensor components[4, 9]. The sdpf-m[10] and GXPF1J[11] interactions are used for *sd*-shell and *fp*-shell part, respectively, while the VMU is adopted for the *sd*-*fp* cross shell part. This interaction will be referred as SDPF-VMU. Configurations are restricted within $2\hbar\omega$

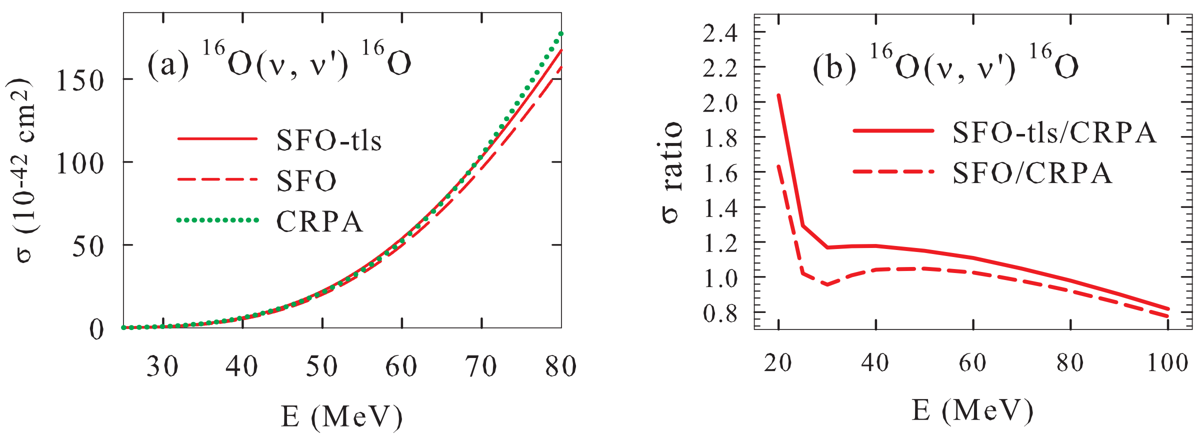

Figure 3. The same as in Fig. 2 for neutral current reaction; ^{16}O (ν, ν') ^{16}O.

excitations, $(sd)^{-2}(fp)^2$, and the GT transition strengths are obtained for SDPF-VMU and WBT[7] interactions with the quenching factor of f =0.775[12]. For SDPF-VMU, the energy of the first 1^+ state of ^{40}K is well reproduced and the strength distribution is also rather well described. Calculated $B(GT_{-})$ and the sum of $B(GT_{-})$ up to the excitation energy of ^{40}K (E_x) are shown in Fig. 4 as well as experimental values obtained by recent (p, n) reaction[13]. In case of WBT, the GT strength distribution is shifted toward lower energy by 1.81 MeV so that the E_x for the first 1^+ state coincides with the experimental value; this case is referred as WBT-ΔE. The experimental GT strength is rather well described by SDPF-VMU as shown in Fig. 4(b). The sum of the GT strength in Ref. [12] is smaller than the observed strength[13].

Calculated cross section for ^{40}Ar (ν, e^-) ^{40}K is shown in Fig. 5 for SDPF-VMU. The GT transitions and the transition to the isobaric analog state (IAS) are included. The contributions from the transitions where the final electron energy is larger than 5 MeV, which is consistent with the experimental condition for ICARUS[14], are taken into account. The calculated cross section is consistent with that obtained from experimental GT strength from the (p, n) reaction[13].

Cross sections folded over ^{8}B ν spectrum[15] are shown in Table I. Here, the contributions from E_1^5 (axial electric dipole), $M1$ (magnetic dipole), C_1^5 (axial Coulomb) and L_1^5 (axial longitudinal) for GT and $C0$ (Coulomb) and $L0$ (longitudinal) for IAS are taken into account, except for the case of Ref. [12] where only the E_1^5 and $C0$ contributions are included. Note that $C0 + L0 = (\frac{q^2-\omega^2}{q^2})^2 C0$ with q (ω) the momentum (energy) transfer. The GT contributions are found to be enhanced for SDPF-VMU and WBT-ΔE about by 40% compared with those of Ref. [12].

4. Electron Capture Reactions in Ni Isotopes

Electron capture reactions in Ni isotopes in stellar environments are studied by using the new shell model Hamiltonian, GXPF1J[11]. Spin properties of fp-shell nuclei are well described by GXPF1J with the universal quenching factors; g_A^{eff}/g_A =0.74 and g_s^{eff}/g_s =0.75. Experimental GT_+ strengths in the β^+ channel in ^{58}Ni [16] and ^{60}Ni [17] are well reproduced by GXPF1J [18]. Thus, the electron capture rates in ^{58}Ni and ^{60}Ni obtained from the experimental GT_+ strengths

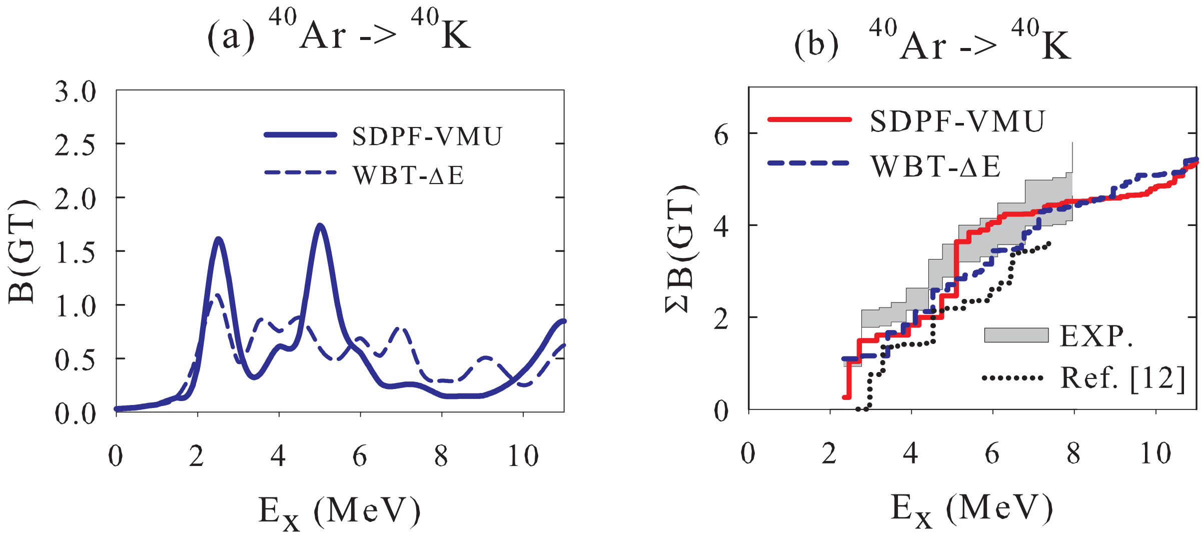

Figure 4. (a) GT strengths for ^{40}Ar $\rightarrow$ ^{40}K transition obtained by shell model calculations with the use of SDPF-VMU and WBT-ΔE interactions. (b) The sum of $B(GT)$ values up to excitation energy E_x of ^{40}K for SDPF-VMU and WBT-ΔE as well as the experimental data[13]. The values in Ref. [12] are also shown.

Table 1. Calculated cross sections for ^{40}Ar (ν, e^-) ^{40}K reaction folded over the neutrino spectrum of ^{8}B[15]. Contributions from GT, IAS and GT+IAS transitions are shown in units of 10^{-43}cm^2 for SDPF-VMU, WBT-ΔE interactions and Ref. [12].

	GT	IAS	GT+IAS
SDPF-VMU	10.99	2.10	13.1
WBT-ΔE	10.78	2.10	12.9
Ref. [12]	7.7	3.8	11.5

are well reproduced by GXPF1J at high temperatures, $T = T_9 \times 10^9$ K with $T_9 = 1\sim10$, and at high densities, $\rho Y_e = 10^7 \sim 10^{10}$ g/cm^3 with Y_e the lepton-to-baryon ratio in stars[18]. The GXPF1J is also promissing in neutron-rich Ni isotopes. The capture rates in ^{56}Ni for GXPF1J are found to be smaller compared to those for KB3G [19] due to larger fragmentation of the GT strength for GXPF1J. The extension of the present work to other isotopes such as Co and Mn is now under way[20].

The authors would like to thank B. Balantekin for raising the problem of ^{13}C contamination. The shell model calculations were carried out by the codes OXBASH[21] and MSHELL64[22]. This work has been supported in part by Grants-in-Aid for Scientific Research (C)22540290 of the Ministry of Education, Culture, Sports, Science and Technology of Japan.

References

[1] Suzuki T, Fujimoto R and Otsuka T 2003 *Phys. Rev.* C **67** 044302
[2] Suzuki T and Otsuka T 2008 *Phys. Rev.* **78** 061301(R)

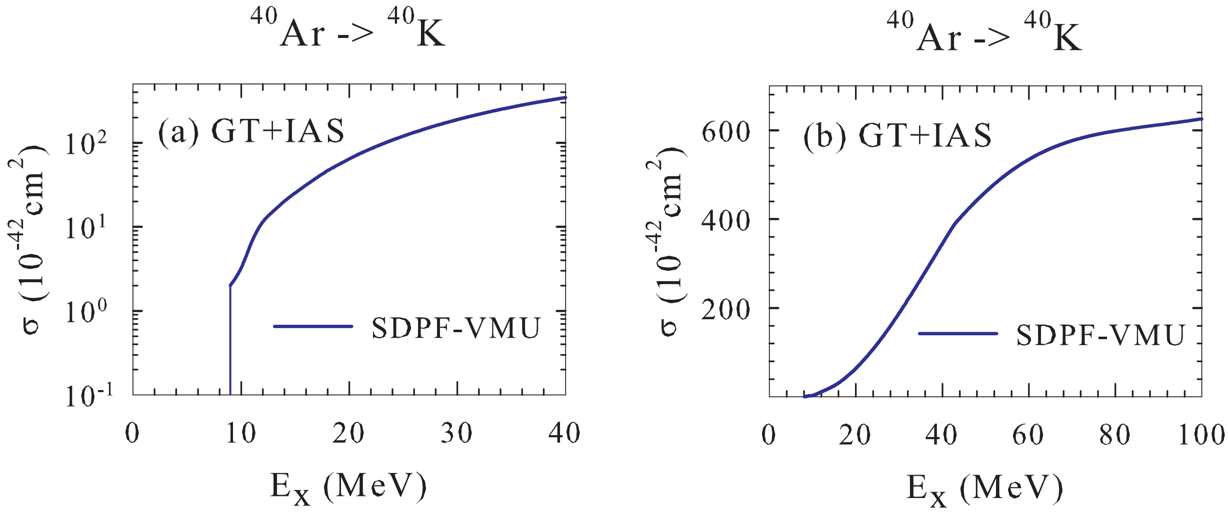

Figure 5. Calculated reaction cross sections for ^{40}Ar (ν, e^-) ^{40}K reaction obtained by shell model calculations with the use of SDPF-VMU. The GT and IAS transitions are taken into account. Results are shown up to E_x = (a) 40 MeV (log scale) and (b) 100 MeV.

[3] Honma M, Otsuka T, Brown B A and Mizusaki T 2002 *Phys. Rev.* C **65** 061301(R); 2004 ibid. **69** 034335
[4] Otsuka T, Suzuki T, Honma M, Utsuno Y, Tsunoda N, Tsukiyama K and Hjorth-Jensen M 2010 *Phys. Rev. Lett.* **104** 012501
[5] Suzuki T, Chiba S, Yoshida T, Kajino T and Otsuka T 2006 *Phys. Rev.* C **74** 034307
[6] Yoshida T, Suzuki T, Chiba S, Kajino T, Yokomakura H, Kimura K, Takamura A and Hartmann D H 2008 *Astrophys. J.* **686** 448
[7] Warburton E K and Brown B A 1992 *Phys. Rev.* C **46** 923
[8] Kolbe E, Langanke K and Vogel P 2002 *Phys. Rev.* D **66** 013007
[9] Otsuka T, Suzuki T, Fujimoto R, Grawe H and AkaishiY 2005 *Phys. Rev. Lett.* **95**, 232502
[10] Utsuno Y, Otsuka T, Mizusaki T and Honma M 1999 *Phys. Rev.* C **60** 054315
[11] Honma M et al. 2005 *J. Phys. Conf. Ser.* **20** 7
[12] Ormand W E, Pizzochero P M, Bortignon P F and Broglia R A 1995 *Phys. Lett.* **B345** 343
[13] Bhattacharya M, Goodman C D and Garcia A 2009 *Phys. Rev.* C **80** 055501
[14] Bachall J N, Baldo-Ceolin M, Cline C B and Rubbia C 1986 *Phys. Lett.* **B178** 324
[15] Winter W T et al. 2003 *Phys. Rev. Lett.* **91** 252501
[16] Hagemann M et al. 2004 *Phys. Lett.* B **579** 251
[17] Anantaraman et al. 2008 *Phys. Rev.* C **78** 065803
[18] Suzuki T, Honma M, Mao H, Otsuka T and Kajino T 2011 *Phys. Rev.* C **83** 044619
[19] Caurier E et al. 2005 R̂ev. Mod. Phys. **77** 427
[20] Suzuki T, Honma M, Yoshida T, Mao H, Kajino T and Otsuka T 2011 *Prog. Part. Nucl. Phys.* **66** 385
[21] OXBASH, The Oxford, Buenos-Aires, Michigan State, Shell Model Program, Brown B A, Etchegoyen A and Rae W D M 1986 *MSU Cyclotron Laboratory Report* No. 524
[22] Mizusaki T, Shimizu N, Utsuno Y and Honma M 2010, unpublished.